Growth Study and Theoretical Investigation of the Ultrathin Oxide SiO_2-Si Heterojunction

Alexander A. Demkov[1,*] and Otto F. Sankey[2]
[1]*Predictive Engineering Laboratory, Motorola, Inc., Mesa, Arizona 85202*
[2]*Department of Physics and Astronomy, Arizona State University, Tempe, Arizona 85287*
(Received 10 March 1999)

The local atomic structure of ultrathin gate oxides and its effect and that of the corresponding SiO_2-Si interface on the band offset of a MOS structure are investigated theoretically. To generate a physically realistic interface, we perform a "direct oxidation" simulation using quantum molecular dynamics. The critical thickness at which the oxidation rate switches from being limited by chemical kinetics to being diffusion limited is estimated. A novel method is introduced to evaluate the band offset within local orbital density functional theory. The valence band offset for the ultrathin oxide is found to be smaller (by 0.3 eV) than that of oxides thicker than $\sim$10 Å in accord with the recent XPS results.

PACS numbers: 73.40.Kp, 81.65.Mq

We describe a consistent methodology to create a realistic atomic geometry of the SiO_2-Si heterojunction, and to determine its properties such as the valence band offset. The oxide-silicon interface is the basis for CMOS (complementary metal-oxide semiconductor) technology which is ubiquitous in all of modern electronics. The rapid scaling of CMOS devices in industry to ever smaller dimensions drives us to seek a better understanding of this system at the microscopic level. The atomic structure of ultrathin oxides of a few angstrom thickness and the interface itself are currently being studied by a range of surface-science techniques [1]. Impressive progress has been made, yet significant gaps in our understanding remain. For example, reliable theoretical predictions including interface dipole contributions of the valence band offset are not possible if the local structure near the interface is undetermined.

The conventional method to simulate an interfacial structure for theoretical analysis is to fuse the two most relevant crystalline phases into a slab, and apply periodic boundary conditions. Such an approach was used by Herman [2] to investigate the SiO_2-Si cristobalite-diamond interface. More recently Hane *et al.* [3] and Pasquarello *et al.* [4] have studied this system using energy minimization techniques to allow the rearrangement of interatomic bonds at the interface to generate a more realistic local structure. One drawback of such a strategy is that the sharpness of the interface is built-in by construction. In this paper, we present a method which simulates physical growth, and we construct a SiO_2-Si interface of a few oxide layers by a direct quantum molecular dynamics oxidation of the Si(001) surface. We use a simplified self-consistent density functional theory quantum molecular dynamics method as developed in Fireball96 [5], which employs a local orbital minimal sp^3 basis of slightly excited pseudoatomic orbitals [6]. Hard pseudopotentials and a local exchange correlation are used. The method has been successfully demonstrated on a variety of materials problems [7], including oxides and zeolites [5]. The major limitation of the method is on systems whose charge density cannot be represented as a summation of fragments, or on noncovalent/nonionic systems with more subtle forms of bonding. Variants and extensions of the approach have been developed by others [8,9].

The initial oxidation of Si(001) has been extensively studied both theoretically and experimentally [10–12]. However, most studies do not go further than the formation of the first oxide layer. Our goal is to study a complete heterojunction of various thicknesses. We grow the oxide by impinging O_2 molecules, one at a time, onto the previously dimerized Si(001). The molecules interact with the surface and an artificial velocity damping is enabled to remove exothermic heat and guide the system towards the energy minimum. We use a 5.43×5.43 Å^2, eight Si layers thick simulation cell (16 Si atoms, one dimer per cell). When the thickness of the grown oxide reaches 7 Å we add four more layers to the bottom of the cell (24 Si atoms). Selected results are checked with a 7.679×7.679 Å^2 cell (two dimers per cell), and 10.86×10.86 Å^2 cell (four dimers per cell). The bottom surface of the slab is dimerized Si(001) and remains inactive during the simulation, as close monitoring of the charge distribution reveals. One special k-point is used for the Brillouin zone sampling in all cases. The details of the oxidation simulation will be reported elsewhere.

We first describe decomposition and incorporation of the first O_2 molecule projected at the surface, which produces two oxygen atoms incorporated into Si-Si bonds (oxygen atoms DB and BB in Fig. 1a). One oxygen atom positions itself into a bridging position in the middle of the surface dimer bond (DB), and the other oxygen atom assumes a bridging position in the middle of a back bond (BB) between the upper dimer atom and the surface. The oxygen atom in the DB position forms two Si-O bonds of 1.58 Å, and the Si-O-Si angle is 134°. The BB oxygen forms two different Si-O bonds of 1.57 and 1.61 Å, and the Si-O-Si angle is 132°. The angle indicates a compressive strain in this "oxide layer," since the Si-O-Si angles are less then 140°–150° typical for (4; 2) networks of silicon

 0031-9007/99/83(10)/2038(4)$15.00

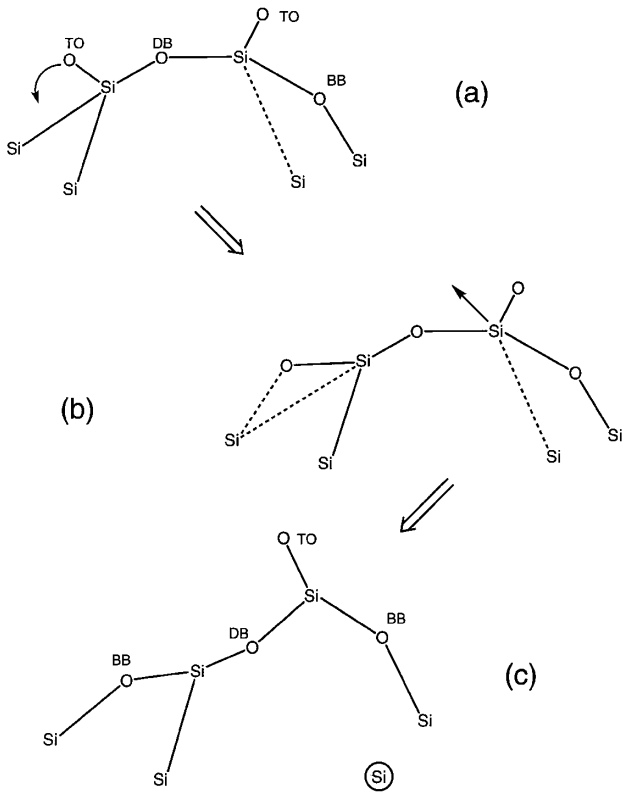

FIG. 1. Schematic of the "peeling" oxidation mechanism. (a) In the starting configuration there are two terminal oxygen atoms (TO), and two bridging oxygens; one bridging oxygen is a dimer bridge (DB), and one is in a back bond position (BB). This results in a Si-Si back bond of the three-oxygen-coordinated upper dimer atom being severely stretched. (b) One terminal oxygen attacks a back bond of the lower dimer atom, and the stretched Si-Si back bond of the upper Si dimer atom breaks off causing the three-oxygen-coordinated upper dimer atom to move away. (c) In the final geometry there are three bridging oxygen atoms, and one terminal. The three-oxygen-coordinated upper Si dimer atom moved away exposing the crystal interior.

dioxide. An interesting feature is that the single remaining Si-Si back bond of the upper dimer is severely stretched to 2.56 Å (dashed line in Fig. 1a). This fact is key to further oxidation as we now show.

We observed the following process for incorporation of the second O_2 molecule. Each of the two oxygen atoms forms bonds with one of the dimer Si atoms which then become terminal atoms. This creates one Si atom three-coordinated by oxygen, and one two-coordinated (Fig. 1a). As the simulation progresses, the oxygen attached to the two-coordinated Si moves towards the bulk and inserts itself into the back bond (Fig. 1b). The Si-Si back bond of the Si atom with three oxygen neighbors (DB, BB, and a terminal oxygen) continues to stretch and is finally broken off (Fig. 1c). The upper dimer is now connected to the surface via two oxygen bridges (DB and BB). It moves upwards as it is being "peeled," leaving behind a hole that exposes the crystal interior four layers below the surface. This peeling appears to be an effective oxidation mechanism that accelerates the layer by layer initial oxidation since it exposes the surface to further chemical attack by oxygen. Briefly, the initial processes involving the first two oxygen molecules are as follows: (i) decomposition of $O_2(1)$ into a back bond and a dimer bond, (ii) catalytic decomposition of $O_2(2)$ by dangling bonds to create a pair of terminal oxygens, and (iii) a cooperative peeling of the surface dimer to expose deeper layers.

Continuing the oxidation to incorporate five oxygen molecules, the typical SiO_2 (4; 2) network emerges. When the thickness of the oxide layer reaches about 7 Å (12 oxygen atoms per 30 $Å^2$) "ballistic oxidation" ceases, and oxygen molecules no longer chemically attack the SiO_2 layer. They are unable to reach the buried silicon underneath, but instead are captured within the oxide. We roughly estimate the density of this "ballistically" grown oxide to be 2.43 g/cm^3. We conclude that at this thickness the oxidation becomes diffusion limited. These results suggest there exists a very fast oxidation step which precedes the Deal-Grove (diffusion limited) growth [13]. The relative constancy of native oxide thicknesses may be the physical manifestation of such a pre–Deal-Grove oxidation.

Our study cannot properly model oxygen diffusion, so we must change our strategy to continue growth. We now place oxygen molecules, one at a time, on the oxide side of the interface by hand to continue oxidation. The oxide grows under strain since the previously grown oxide layer prevents a complete relaxation. A sample with four oxide layers is shown in Fig. 2. We estimate the density to be $\sim$2.7 g/cm^3 that is slightly higher than that of a thick thermal oxide. One can clearly see the oxide region built of corner sharing tetrahedra, and the interfacial layer with Si atoms in several intermediate oxidation states. The oxide thus grown contains 7-, 8-, and 9-fold rings, and therefore is topologically different from crystalline silica polymorphs. The bond length and angle distributions are shown in Fig. 2. The contribution from the atoms at the interface are indicated with a thin black line, and one can clearly see the strain in this region. This sample does not have any dangling bonds at the interface. However, a high temperature anneal results in a lower energy structure containing Si dangling bonds.

To estimate the resulting valence band discontinuity at the Si-SiO_2 interface, we use a variant of the Van de Walle and Martin [14] method, taking advantage of our local orbital basis. Van de Walle and Martin use an average electron potential as a reference energy against the top of the valence band, ΔE_{RV}, for bulk phases. Instead, we use the average spatial dependence of the expectation value of the Hamiltonian calculated for the valence ($3s$ or $3p$) states of Si, ϵ_s and ϵ_p [$\langle\phi_s(i)|H|\phi_s(i)\rangle$ and $\langle\phi_p(i)|H|\phi_p(i)\rangle$, respectively] [15]. In the following, we will use ϵ_s as the reference energy, but similar results are obtained using ϵ_p. The valence band offset, Δ_{VBO}, is obtained from

$$\Delta_{\mathrm{VBO}} = \epsilon_s(\mathrm{Si}) + \Delta E_{\mathrm{RV}}(\mathrm{Si}) - \epsilon_s(\mathrm{SiO_2}) - \Delta E_{\mathrm{RV}}(\mathrm{SiO_2}), \quad (1)$$

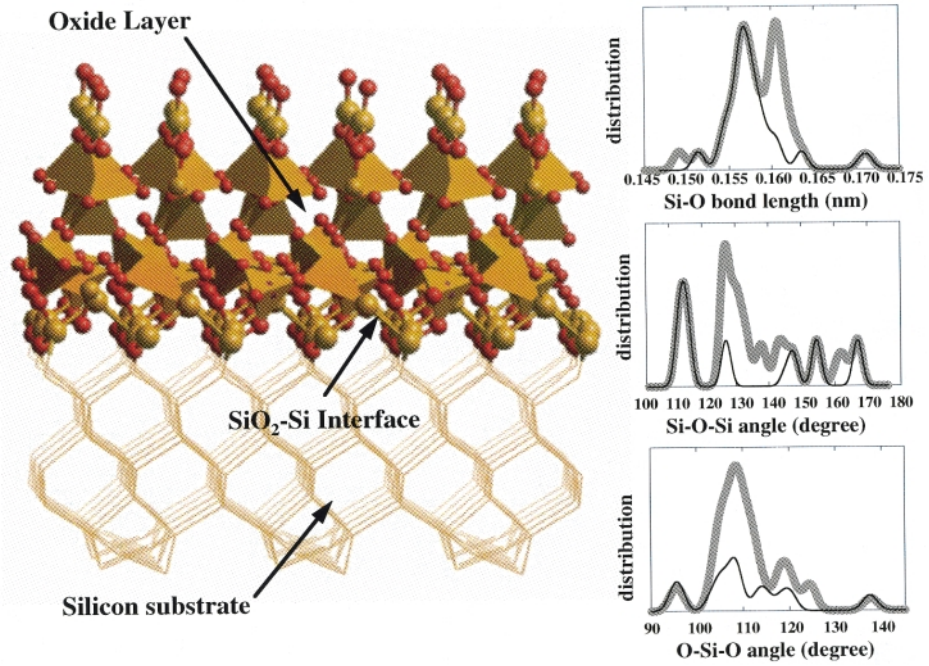

FIG. 2 (color). The structural model of a Si-SiO_2 heterojunction. The ultrathin 8 Å oxide layer is separated from the underlying Si substrate by 4 Å of the interface (12 Å total). The inset shows the bond length and angle distributions in the sample. Contributions from the atoms at the interface are indicated with a thin black line. One can see that deviations from the typical silica values are localized in the interfacial layer.

where $\epsilon_s(\mathrm{Si})$ and $\epsilon_s(\mathrm{SiO_2})$ are the reference levels in Si and SiO_2, respectively, and $\Delta E_{\mathrm{RV}}(i)$ is the energy difference between $\epsilon_s(i)$ and the top of the valence band edge in bulk material i. For bulk Si, $\Delta E_{\mathrm{RV}}(\mathrm{Si})$ is 8.31 eV. The determination of $\Delta E_{\mathrm{RV}}(\mathrm{SiO_2})$ will be discussed below.

In Fig. 3 we show ϵ_s for Si atoms in our model heterojunction along the z direction perpendicular to the plane of the interface (Si, left; SiO_2, right). Crosses correspond to the "as grown" sample, and diamonds to the same sample after it was "annealed." One can see three regions. (i) In the Si layer (left), ϵ_s is near -13 eV corresponding to the oxidation state Si^0. (The data point on the extreme left is the inactive lower reconstructed surface.) This places the valence band top near -5 eV. (ii) In the oxide (right), ϵ_s values near -20 eV are characteristic of nominal Si^{4+}. (iii) In between these two regions (for distance values near 0) there is a 4 Å interfacial region where Si is in intermediate oxidation states. For the annealed sample (diamonds) we also have a defect Si with two dangling bonds ($\epsilon_s \sim -12.5$ eV). We can now establish the reference energy level on both sides of the interface. In the oxide layer the reference layer is at -19.8 ± 0.2 eV.

The remaining unknown in Eq. (1) is $\Delta E_{\mathrm{RV}}(\mathrm{SiO_2})$, which determines where to place the top of the valence band in the oxide layer. The value of $\Delta E_{\mathrm{RV}}(\mathrm{SiO_2})$ will vary from one SiO_2 polymorph to another, and our layer does not correspond to any crystalline polymorph. It is well known that core level shifts depend on Si-O bond length and to a lesser degree on bond angles. One might expect a similar dependence for the valence levels (ϵ_s, ϵ_p) as well as for the valence band top. The structure of β-cristobalite offers a convenient vehicle to investigate how $\Delta E_{\mathrm{RV}}(\mathrm{SiO_2})$ depends on bond lengths and angles since Si-O bond lengths and Si-O-Si bond angles can be independently varied without constraints. We find that $\Delta E_{\mathrm{RV}}(\mathrm{SiO_2})$ is well described by a linear function of bond length d_{SiO} as

$$\Delta E_{\mathrm{RV}}(\mathrm{SiO_2}) = -11.4 d_{\mathrm{SiO}}\ \mathrm{eV/\AA} + 28.03\ \mathrm{eV}. \quad (2)$$

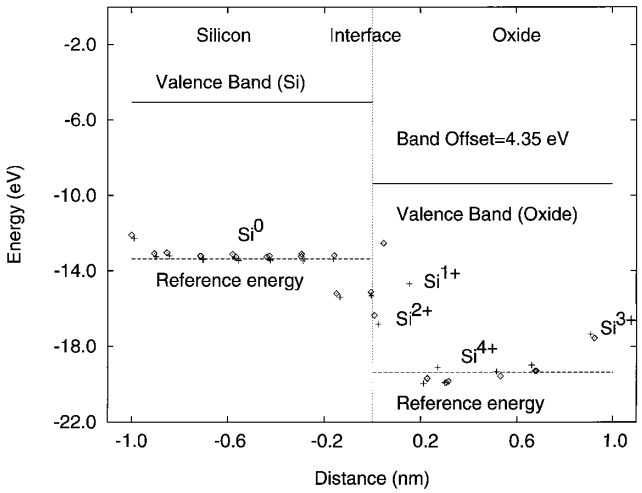

FIG. 3. The Si 3s valence state matrix element ϵ_s plotted across the model heterojunction shown in Fig. 2. Crosses correspond to the "as grown" sample, and diamonds correspond to the "annealed" sample. There are no dangling bonds in the "as grown" structure. One can clearly see the interfacial region between -0.2 and 0.2 nm. The different oxidation states of Si are indicated.

The dependence of $\Delta E_{\mathrm{RV}}(SiO_2)$ on Si-O-Si angle is weak for angles in the range from 130° to 180°, and we shall neglect it in the analysis.

It is now possible to place the top of the valence band in the oxide layer using Eq. (2) and an average Si-O bond length in the oxide layer. For the thin oxide layer (8 Å) shown in Fig. 2, we obtain a valence band offset of 4.35 eV, and the alignment diagram is shown in Fig. 3. For a thicker oxide layer (12 Å, not shown), we obtain 4.65 eV in remarkable agreement with the experimental value of 4.7 eV for conventional oxides [16].

It is important to recognize that there are two quantities in our computational procedure that define the valence band offset. One is $\epsilon_s(\mathrm{Si}) - \epsilon_s(SiO_2)$, which takes into account the interfacial dipole. The second one is $\Delta E_{\mathrm{RV}}(SiO_2)$ that is determined by the local atomic structure of the oxide. A small change in the average Si-O bond length results in a measurable difference in the offset due to a large slope (−11.4 eV/Å) of $\Delta E_{\mathrm{RV}}(SiO_2)$ in Eq. (2). It is instructive to compare two samples of the same thickness but with different interfaces and Si-O bond length distributions. We compare the as grown and annealed samples shown in Fig. 3. For the as grown sample, we find $\epsilon_s(\mathrm{Si}) - \epsilon_s(SiO_2) = 6.06$ eV, $\Delta E_{\mathrm{RV}}(SiO_2) = 10.02$ eV, and $\Delta_{\mathrm{VBO}} = 4.35$ eV, and for the annealed sample we obtain $\epsilon_s(\mathrm{Si}) - \epsilon_s(SiO_2) = 6.44$ eV, $\Delta E_{\mathrm{RV}}(SiO_2) = 9.90$ eV, and $\Delta_{\mathrm{VBO}} = 4.85$ eV. Somewhat surprising is that the difference in $\epsilon_s(\mathrm{Si}) - \epsilon_s(SiO_2)$ (influenced by the interfacial dipole) accounts for 80% of the 0.50 eV change in the offset. Similarly, the 0.3 eV difference obtained for the thinner and thicker oxides above is mainly due to $\epsilon_s(\mathrm{Si}) - \epsilon_s(SiO_2)$.

Recently Nohira *et al.* [16] have investigated the valence band discontinuity at the Si-SiO_2 interface with *in situ* x-ray photoemission spectroscopy. The changes in the valence band are monitored during the oxidation, and the thickness dependence is studied. It is found that for oxides thinner than a critical thickness of 9 Å, the valence band offset is 0.2 eV smaller than that for a thicker oxide. The change in the band offset at the critical thickness is rather abrupt. Nohira *et al.* assumed that the offset does not depend on the interface structure. Their results are, in fact, consistent with the structure of the oxide changing slightly near 8–10 Å. At this thickness, the oxidation switches from ballistic oxidation limited only by the rate of the chemical reaction to one that is diffusion limited oxidation. This change likely affects future growth and hence the structure of the oxide. Since we have shown that the band offset sensitively depends on the bond length distribution in the oxide layer, only a 0.02 Å change in the average bond length results in over a 0.2 eV change in the band offset. Such a subtle change in the structure of the oxide need not result in a different density of oxidation states, and may manifest itself in the sudden jump of the band offset at 10 Å reported by Nohira *et al.* [16]. However, as we have shown, a change in the interfacial dipole results in an even larger change.

In conclusion, we report a theoretical investigation of the Si-SiO_2 heterojunction. A direct molecular dynamics oxidation is used to successfully generate a physical interface structure and an ultrathin oxide layer. A "peeling" oxidation mechanism is observed at the very early stages of oxidation which exposes the crystal interior. A pre–Deal-Grove oxidation regime of "ballistic" oxidation for oxides thinner than 7–10 Å is suggested. This change in the growth mechanism results in a change of the oxide structure and a 0.3 g/cm^3 change in density in qualitative agreement with experiment [17]. A new method, for local orbital techniques, is used to estimate the band offset at the interface. A simple correlation between the oxide layer bonding structure (bond lengths) and the valence band offset at the silicon-oxide interface is suggested. Our results may provide an explanation for a difference in the band offset between ultrathin oxides (less than 10 Å thick) and conventional oxides.

We thank T. Lenosky, S. Zollner, P. Tobin, E. Hall, and A. Korkin for stimulating discussions and support of our work. O. F. S. thanks NSF (DMR 95-26274) for its support.

*Email address: Alex.Demkov@motorola.com

[1] T. Engel, Surf. Sci. Rep. **18**, 91 (1993).
[2] F. Herman and R. V. Kasowski, J. Vac. Sci. Technol. **19**, 395 (1981).
[3] M. Hane, Y. Miyamoto, and A. Oshiyama, Phys. Rev. B **41**, 12 637 (1990).
[4] A. Pasquarello, M. S. Hybertsen, and R. Car, Appl. Phys. Lett. **68**, 625 (1996).
[5] A. A. Demkov, J. Ortega, O. F. Sankey, and M. P. Grumbach, Phys. Rev. B **52**, 1618 (1995).
[6] O. F. Sankey and D. J. Niklewski, Phys. Rev. B **40**, 3979 (1989).
[7] O. F. Sankey, A. A. Demkov, W. Windl, J. H. Fritsch, J. P. Lewis, and M. Fuentes-Cabrera, Int. J. Quantum Chem. **69**, 327 (1998).
[8] A. P. Horsfield, Phys. Rev. B **56**, 6594 (1997).
[9] P. Pou, R. Perez, J. Ortega, and F. Flores, Mater. Res. Soc. Symp. Proc. **491**, 91 (1998).
[10] Y. Miyamoto and A. Oshiyama, Phys. Rev. B **43**, 9287 (1991); **44**, 5931 (1991).
[11] T. Uchiyama and M. Tsukada, Phys. Rev. B **55**, 9356 (1997).
[12] M. Weldon, B. B. Stefanov, K. Raghavachari, and Y. I. Chabal, Phys. Rev. Lett. **79**, 2851 (1997).
[13] B. E. Deal and A. S. Grove, J. Appl. Phys. **36**, 3730 (1965).
[14] C. G. Van de Walle and R. M. Martin, Phys. Rev. B **35**, 8154 (1987).
[15] The Hamiltonian matrix elements are sensitive to the local environment and long-range Coulomb forces.
[16] H. Nohira, A. Omura, M. Katayama, and T. Hattori, Appl. Surf. Sci. **123/124**, 546 (1998).
[17] E. Hasegawa, A. Ishitani, K. Akimoto, M. Tsukiji, and N. Ohta, J. Electrochem. Soc. **142**, 273 (1995).